

Towards External Sensor based Simultaneous Magnetic Actuation and Localization for WCE

Yangxin Xu, Ziqi Zhao, Keyu Li and Max Q.-H. Meng*, *Fellow, IEEE*

Abstract—This paper presents a close-loop simultaneous acceleration and localization system for the wireless capsule endoscopy inside the intestine for clinical applications. A compact capsule with two embedded magnetic rings is actuated by an external rotating magnet, and the magnetic fields of the three magnets are measured by an external sensor array. In the proposed workflow, the magnetic field of the external magnet is first eliminated using an Integral Filter based strategy. Then the magnetic field of the moving capsule is modeled to generate an estimation of its pose. The fusion of the actuation and localization steps are implemented using an Unscented Kalman Filter. The proposed method is validated through experiments on phantoms and animal organs. The localization accuracy of the capsule reaches 5.5mm and 5.2° for position and orientation, respectively.

Index Terms—Simultaneous Magnetic Actuation and Localization, Integral Filter, Wireless Capsule Endoscopy.

I. INTRODUCTION

Wireless Capsule Endoscopy (WCE) is a technology designed to perform imaging of the entire Gastrointestinal (GI) tract of patients in a non-invasive manner. [1]. However, although lesions could be detected from the captured images, it is difficult to locate the accurate position of the lesions, which may delay the follow-up treatment. Furthermore, since the capsule moves passively inside human body without control or actuation, the whole imaging process in the clinical applications could take up to about 8 ~ 12 hours.

Among the magnetic field based localization systems for WCE, many methods were proposed based on an external sensor array to simplify the internal structure of the capsule. By placing a single magnet in the capsule, the 5-D pose of the capsule can be calculated from the sampled magnetic field [2][3]. In order to obtain the 6-D pose of the capsule, other designs of the capsule with two mutually perpendicular or opposite magnets placed inside are proposed [4][5]. These methods can provide the real-time capsule localization, but autonomous actuation of the capsule is not available.

The close-loop magnetic actuation and localization technology for WCE have been explored recently to integrate the

Y. Xu, Z. Zhao and K. Li are with the Department of Electronic Engineering, The Chinese University of Hong Kong, Hong Kong SAR (e-mail: yxxu@ee.cuhk.edu.hk).

Max Q.-H. Meng is with the Department of Electronic Engineering, The Chinese University of Hong Kong, Hong Kong SAR, and the Shenzhen Research Institute of the Chinese University of Hong Kong in Shenzhen, China (e-mail: max.meng@ieee.org).

*Corresponding author.

actuation and localization processes. [6] reviews the previous studies in this field. Generally, the capsule is designed with a permanent passive magnet placed inside and is actuated by an external permanent magnet. One of the biggest challenges of the close-loop magnetic actuation and localization is that the use of magnetic sources for both actuation and localization purposes may result in undesired interferences with the localization system [6]. In some studies, the actuation and localization are separated into two steps [7][8]. This could effectively eliminate the negative effect of the actuation magnetic field to the localization system, but would result in a decline in the actuation efficiency, since the actuation device is turned off during the localization process. Therefore, the Simultaneous Magnetic Actuation and Localization is proposed to overcome the problem. Some researchers designed the capsule with a special structure of the passive magnet and embedded sensors to eliminate the undesired magnetic field of the passive magnet for localization purpose. Then the capsule is actuated by a moving permanent magnet with an electromagnet fixed around it [9]. However, such methods actuate the capsule by directly pulling the capsule by magnetic force. Due to the fact that the magnitude of magnetic force decreases much faster than that of magnetic torque when the distance between two magnets increases [10], this actuation strategy is only effective in a very limited distance. Therefore, many researchers switched to develop methods based on rotating actuation [10][11]. A first system for simultaneous magnetic localization and actuation using a single rotating magnet was proposed in [12]. However, the specially designed embedded magnet and sensors will occupy too much space in the capsule, making it difficult to put in other functional modules such as the imaging and communication modules. Therefore, such capsule design is unacceptable in clinical use.

Inspired by the external sensor array designed in the localization system [2], in order to both actuate the capsule efficiently and make the capsule more compact, we propose to take advantage of the rotating actuation and use an external sensor based localization method to build a close-loop system for simultaneous actuation and localization for WCE. The two issues to be solved are as follows:

- In the external sensor based localization systems, only the magnetic field of the capsule is sampled by the sensor array. However, in our application scenario, both

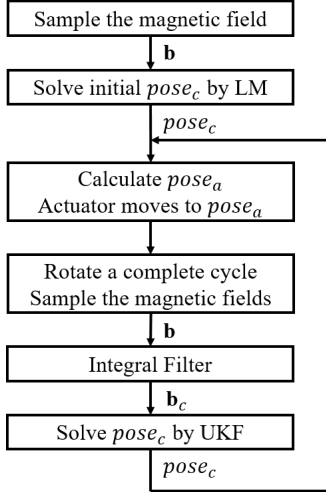


Fig. 1. Before the actuator begins to rotate, the initial 6-D pose of the capsule $pose_c$ is solved from the static magnetic field. Then the actuator moves to $pose_a$, which is calculated according to $pose_c$. The magnetic fields of both the actuation magnet and magnetic rings are sampled while the actuation magnet rotates for one revolution. The integral filter is introduced to eliminate the magnetic field of the actuator, then the new pose $pose_c$ of the capsule is updated by the Unscented Kalman Filter (UKF) to close the actuation-localization loop.

the magnetic fields of the actuation magnet and the capsule are measured. Therefore, the magnetic field of the actuation magnet should be eliminated firstly to avoid undesired interferences.

- A motion model of the moving capsule in the actuation and localization steps needs to be established to estimate the pose of the capsule, and a strategy should be proposed to fuse the actuation and localization steps to realize the close-loop control.

In this paper, we address the first issue by exploiting the motion mode of the actuation magnet and introducing an *Integral Filter* (IF) based method to eliminate the magnetic field of the external actuation magnet. The proposed workflow of the system is shown in Fig. 1. The initial 6-D pose of the capsule is solved by Levenberg-Marquard (LM) algorithm. For each revolution of the rotating actuation magnet around its axis (see Fig. 2), the sampling results of the total magnetic fields are input to the Integral Filter to eliminate the magnetic field of the actuation magnet, then the new pose of the capsule is solved from the remaining magnetic field using a motion estimation model with the Unscented Kalman Filter (UKF). The above steps are repeated to accomplish the close-loop actuation and localization of the capsule.

The main contributions of this work are three-fold:

- This is the first feasible study of simultaneous magnetic actuation and localization for WCE using the external sensor array and rotating actuation.
- A novel method which exploits the motion mode of the actuator and introduces the Integral Filter is proposed to eliminate the magnetic field of the actuation magnet.

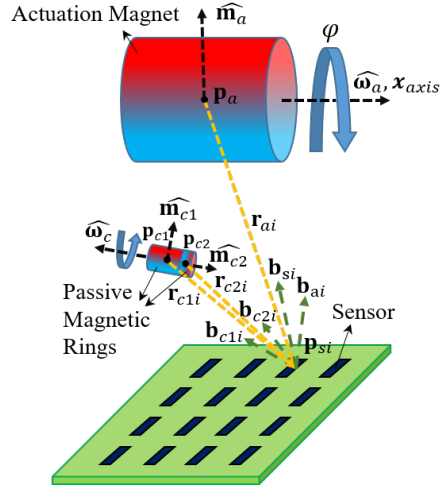


Fig. 2. The total magnetic fields (\mathbf{b}_{si}) of both actuation magnet and magnetic rings are sampled at the i -th sensor. The undesired magnetic field (\mathbf{b}_{ai}) of the actuation magnet is eliminated by the Integral Filter based method, so the remaining magnetic field is the magnetic field ($\mathbf{b}_{c1i} + \mathbf{b}_{c2i}$) generated by the capsule.

- A capsule motion model is established to estimate the pose of the moving capsule.

The rest of this paper is organized as follows. In Section II, the proposed close-loop simultaneous magnetic actuation and localization (SMAL) method is presented in details. The experiments and results are presented in Section III, before we draw some conclusions in Section IV.

II. METHOD

A. Integral Filter

As shown in Fig. 2, the total magnetic fields generated by both the actuation magnet and the passive magnetic rings are sampled by the external sensor array. At time t , the magnetic field of the actuation magnet at the i -th sensor is represented as $\mathbf{b}_{ai}(t)$, and the magnetic fields of the two passive magnetic rings at the i -th sensor are represented as $\mathbf{b}_{c1i}(t)$ and $\mathbf{b}_{c2i}(t)$, respectively. The magnetic field $\mathbf{b}_{si}(t)$ sampled at the i -th sensor can be represented by:

$$\mathbf{b}_{si}(t) = \mathbf{b}_{ai}(t) + (\mathbf{b}_{c1i}(t) + \mathbf{b}_{c2i}(t)) \quad (1)$$

where $\mathbf{b}_{ai}(t), \mathbf{b}_{c1i}(t), \mathbf{b}_{c2i}(t), \mathbf{b}_{si}(t) \in \mathbb{R}^{3 \times 1}$. According to the magnetic dipole model [2], the magnetic field \mathbf{b}_{ai} of the actuation magnet can be calculated with:

$$\mathbf{b}_{ai}(\mathbf{r}_{ai}, \hat{\mathbf{m}}_a) = \frac{\mu_0 \|\mathbf{m}_a\|}{4\pi \|\mathbf{r}_{ai}\|^5} (3\mathbf{r}_{ai}\mathbf{r}_{ai}^T - \mathbf{r}_{ai}^T \mathbf{r}_{ai} \cdot \mathbf{I}_3) \hat{\mathbf{m}}_a \quad (2)$$

where $\hat{\mathbf{m}}_a \in \mathbb{R}^{3 \times 1}$ is the unit magnetic moment, $\mathbf{r}_{ai} \in \mathbb{R}^{3 \times 1}$ indicates the vector from the actuation magnet's center $\mathbf{p}_a \in \mathbb{R}^{3 \times 1}$ to the i -th sensor position $\mathbf{p}_{si} \in \mathbb{R}^{3 \times 1}$, \mathbf{I}_3 represents 3×3 identity matrix, the constant μ_0 is the vacuum permeability, and the constant $\|\mathbf{m}_a\|$ is the magnitude of magnetic moment, which is relevant to the material and volume of the magnet.

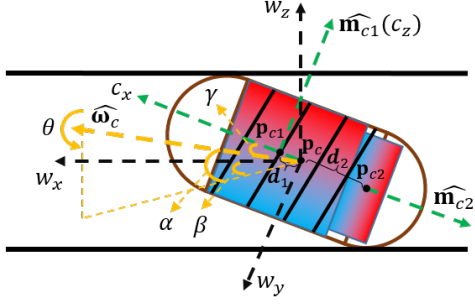


Fig. 3. The capsule is rotating around its moving direction $\widehat{\omega}_c$ at a slanting angle of γ to its heading direction c_x . \mathbf{p}_c represents the position of the capsule. θ represents the angle of rotation around $\widehat{\omega}_c$, and α and β describe the moving direction of the capsule.

For convenience of representation and calculation, as shown in Fig. 2, we assume that the actuation magnet is placed horizontally above the sensor array and rotates around the x-axis, so we set $\widehat{\mathbf{m}}_a = (0 \cos \varphi \sin \varphi)^T$, $\varphi \in [0, 2\pi]$. We set $\widehat{\mathbf{r}}_{ai} = (a \ b \ c)^T$, $a^2 + b^2 + c^2 = 1$, where $\widehat{\mathbf{r}}_{ai}$ is the unit vector of \mathbf{r}_{ai} . Therefore, the magnetic field at point \mathbf{P}_{si} can be calculated by (2), and the result can be written as:

$$\mathbf{b}_{ai}(\varphi) = \frac{\mu_0 \|\mathbf{m}_a\|}{4\pi \|\mathbf{r}_{ai}\|^3} \begin{pmatrix} 3ab \cos \varphi + 3ac \sin \varphi \\ (3b^2 - 1) \cos \varphi + 3bc \sin \varphi \\ 3bc \cos \varphi + (3c^2 - 1) \sin \varphi \end{pmatrix} \quad (3)$$

The integral with respect to degree φ (time t) of (3) on the interval $[0, 2\pi]$ ($[0, T]$) is calculated as:

$$\int_0^{2\pi} \mathbf{b}_{ai}(\varphi) d\varphi = 0 \Rightarrow \int_0^T \mathbf{b}_{ai}(t) dt = 0, \quad (4)$$

which means at any point, the integral of the magnetic fields generated by a rotating magnet during one revolution is 0. Therefore, the magnetic field of the actuation magnet can be eliminated by doing the integration after each spin of the rotating actuation magnet. By integration, (1) changes to:

$$\int_0^T \mathbf{b}_{si}(t) dt = 0 + \int_0^T (\mathbf{b}_{c1i}(t) + \mathbf{b}_{c2i}(t)) dt \quad (5)$$

B. Capsule Motion Model

As discussed in Part A, it is possible to eliminate the effect of the magnetic field formed by the actuation magnet to the localization process by calculating the integral in one revolution. Since the capsule is in motion during this period, the pose of the capsule should be estimated by properly modeling the rotating motion of the capsule. Through a set of experiments, we observe that the capsule basically keeps rotating around an axis at a certain angle to its heading direction. The rotating axis is then defined as the moving direction which can represent the average orientation of the capsule during one revolution. The motion model of the rotating capsule in the localization and actuation steps is established as follows.

1) Localization Step: In Fig. 3, the position of the capsule is $\mathbf{p}_c \in \mathbb{R}^{3 \times 1}$, and the capsule rotates around the moving direction $\widehat{\omega}_c$ at a slanting angle γ to its heading direction. θ represents the angle of rotation around $\widehat{\omega}_c$. α and β describe the moving direction of the capsule. The original capsule x-axis c_x and z-axis c_z ($\widehat{\mathbf{m}}_{c1}$) are along the world x-axis w_x and z-axis w_z , respectively. The rotation matrix of the capsule can be calculated as:

$$\mathbf{R} = \mathbf{R}_z(\beta) \mathbf{R}_y(-\alpha) \mathbf{R}_x(\theta) \mathbf{R}_y(-\gamma) \quad (6)$$

where the \mathbf{R}_x , \mathbf{R}_y , \mathbf{R}_z represent the rotation around the w_x , w_y , w_z axis, respectively. The head direction c_x of the capsule is represented as:

$$c_x = \mathbf{R} \cdot (1 \ 0 \ 0)^T \quad (7)$$

The positions of two passive magnetic rings are:

$$\begin{aligned} \mathbf{p}_{c1} &= \mathbf{p}_c + d_1 \cdot c_x \\ \mathbf{p}_{c2} &= \mathbf{p}_c - d_2 \cdot c_x \end{aligned} \quad (8)$$

where d_1 and d_2 are the distances from the two centers of the two magnetic rings to the center of the capsule. The unit magnetic moments of the two magnetic rings are:

$$\widehat{\mathbf{m}}_{c1} = \mathbf{R} \cdot (0 \ 0 \ 1)^T, \quad \widehat{\mathbf{m}}_{c2} = -c_x \quad (9)$$

Since $\theta \in [0, 2\pi]$, suppose the theoretical capsule magnetic field in one revolution is divided into N parts, the rotation angle θ of the n -th part in one revolution is $2\pi \frac{n}{N}$, and the n -th theoretical magnetic fields ($\mathbf{b}_{c1i}^n, \mathbf{b}_{c2i}^n$) generated by two magnetic rings at the i -th sensor are calculated by (10):

$$\begin{aligned} \mathbf{b}_{c1i}^n &= \frac{\mu_0 \|\mathbf{m}_{c1}\|}{4\pi \|\mathbf{r}_{c1i}\|^5} (3\mathbf{r}_{c1i} \mathbf{r}_{c1i}^T - \mathbf{r}_{c1i}^T \mathbf{r}_{c1i} \cdot \mathbf{I}_3) \widehat{\mathbf{m}}_{c1} \\ \mathbf{b}_{c2i}^n &= \frac{\mu_0 \|\mathbf{m}_{c2}\|}{4\pi \|\mathbf{r}_{c2i}\|^5} (3\mathbf{r}_{c2i} \mathbf{r}_{c2i}^T - \mathbf{r}_{c2i}^T \mathbf{r}_{c2i} \cdot \mathbf{I}_3) \widehat{\mathbf{m}}_{c2} \end{aligned} \quad (10)$$

where the constant μ_0 is the vacuum permeability, and the constant norm ($\|\mathbf{m}_{c1}\|, \|\mathbf{m}_{c2}\|$) is the magnitude of magnetic moment, which is relevant to the material and volume of each magnetic ring. \mathbf{r}_{c1i} and \mathbf{r}_{c2i} are the distances between the two centers ($\mathbf{p}_{c1}, \mathbf{p}_{c2}$) of the two magnetic rings and the position \mathbf{p}_{si} of the i -th sensor, respectively. There are 16 sensors in total, and the integral of the magnetic fields in one revolution at the i -th sensor is calculated as:

$$\sum_{m=0}^M \mathbf{b}_{si}^m = \sum_{n=0}^N (\mathbf{b}_{c1i}^n + \mathbf{b}_{c2i}^n), \quad i \in \{1, 2, \dots, 16\} \quad (11)$$

where the left part of (11) is the integral of sampled magnetic fields in one revolution, and the right part is the integral of theoretical magnetic fields in one revolution. \mathbf{b}_{si}^m represents the m -th sampled magnetic field at the i -th sensor, and M

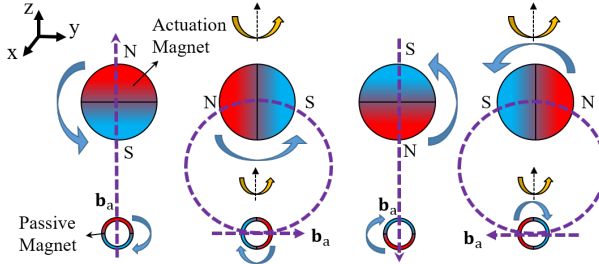


Fig. 4. The schematic diagram of the actuation model. Both the actuator and the capsule can be roughly seen as a cylinder with an axis along the x -direction. The purple dotted line represents the magnetic field line that passes through the capsule. The blue arrows represent the rotation around the x -axis, and the yellow arrows represent the rotation around the z -axis. As illustrated in the 2nd and 4th figures, when the magnetic field line at the capsule is along the y -axis, the capsule will change its orientation with the actuator.

represents the number of sampled magnetic fields in one revolution. The pose ($\mathbf{p}_c, \alpha, \beta, \gamma$) of the capsule can be solved by optimizing the following error function:

$$\begin{aligned} \min_{\mathbf{p}_c, \alpha, \beta, \gamma} & \sum_{i=1}^{16} \left\| \sum_{n=0}^N (\mathbf{b}_{c1i}^n + \mathbf{b}_{c2i}^n) - \sum_{m=0}^M \mathbf{b}_{si}^m \right\| \\ \text{subject to} & -\frac{\pi}{2} < \alpha < \frac{\pi}{2} \\ & 0 \leq \beta < 2\pi \\ & 0 \leq \gamma < \frac{\pi}{2} \end{aligned} \quad (12)$$

2) Actuation Step: As illustrated in Fig. 4, when the magnitude of the magnetic torque is large enough to actuate the capsule, the capsule will rotate synchronously with the actuation magnet. Due to the combined effect of the magnetic force and the magnetic torque, the orientation of the capsule will stay consistent with that of the actuation magnet and move below the actuator. Therefore, the actuation model of the moving capsule can be simply described as:

$$\begin{pmatrix} \mathbf{p}_c^{(t)}[0] \\ \mathbf{p}_c^{(t)}[1] \\ \mathbf{p}_c^{(t)}[2] \\ \alpha_c^{(t)} \\ \beta_c^{(t)} \\ \gamma_c^{(t)} \end{pmatrix} = \begin{pmatrix} \mathbf{p}_a^{(t)}[0] \\ \mathbf{p}_a^{(t)}[1] \\ \mathbf{p}_a^{(t-1)}[2] \\ \alpha_a^{(t)} \\ \beta_a^{(t)} \\ \gamma_a^{(t-1)} \end{pmatrix} \quad (13)$$

where $\mathbf{p}_c^{(t)}, \alpha_c^{(t)}, \beta_c^{(t)}$ and $\gamma_c^{(t)}$ represent the pose $\mathbf{q}_c^{(t)} \in \mathbb{R}^{6 \times 1}$ of the capsule at time t , and $\mathbf{p}_a^{(t)}, \alpha_a^{(t)}$ and $\beta_a^{(t)}$ represent the pose $\mathbf{q}_a^{(t)} \in \mathbb{R}^{5 \times 1}$ of the actuator at time t , so the pose $\mathbf{q}_c^{(t)}$ of the capsule at time t is updated by the previous pose of the capsule $\mathbf{q}_c^{(t-1)}$ and the current pose of the actuator $\mathbf{q}_a^{(t)}$.

C. Close-Loop Control

In the actuation step, the capsule rotates with the active magnet for one revolution, and the pose of the moving capsule is predicted by (13). In the localization step, the pose of the capsule can be updated by (12). We introduce

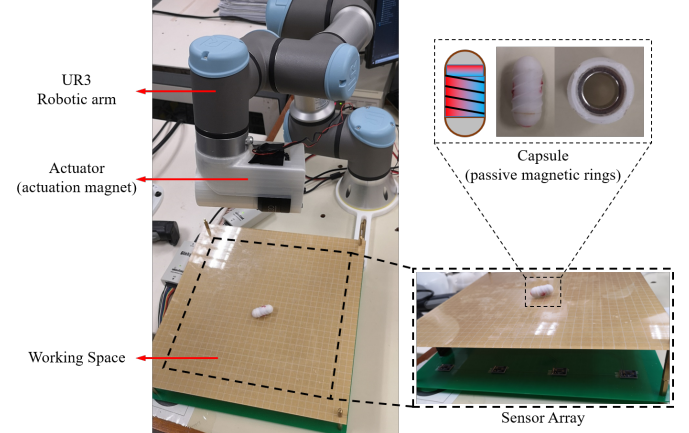


Fig. 5. The presented system setup of the close-loop Simultaneous Magnetic Actuation and Localization (SMAL) for WCE. The actuator consisting of a DC motor and a permanent magnet is mounted at the end-effector of a robotic arm. There are two magnetic rings placed inside the capsule and 16 magnetic sensors in the external sensor array.

the Unscented Kalman Filter (UKF) to fuse the actuation and localization steps. UKF approximates nonlinear functions by key point mapping to find the optimal solution, which makes the calculation simple and efficient.

After fusing the actuation and localization steps, we finally close the actuation-localization loop. The pseudocode of the close-loop SMAL algorithm is generalized in Algorithm 1.

Algorithm 1: Close-Loop SMAL

The first capsule's pose $\mathbf{q}_c^{(0)}$ is initialized by LM algorithm;
 \mathbf{r}_{ca} indicates the preset vector from the capsule to the actuator;

-
- Input:** the past pose $\mathbf{q}_c^{(t-1)}$ of the capsule, the current pose $\mathbf{q}_a^{(t)}$ of the actuator.
Output: the current pose $\mathbf{q}_c^{(t)}$ of the capsule, the new pose $\mathbf{q}_a^{(t+1)}$ of the actuator.
- 1 rotate the actuation magnet for one revolution, while sampling the magnetic fields $\mathbf{b}_{si}^m, i \in \{1, 2, \dots, 16\}, m \in \{1, 2, \dots, M\}$;
 - 2 calculate the integral of the sampled magnetic fields during one revolution: $\sum_{m=0}^M \mathbf{b}_{si}^m$;
 - 3 calculate the integral of the theoretical magnetic fields during one revolution: $\sum_{n=0}^N (\mathbf{b}_{c1i}^n + \mathbf{b}_{c2i}^n)$;
 - 4 UKF actuation step: $\mathbf{q}_c^{(t)}$ is predicted from $\mathbf{q}_c^{(t-1)}$ and $\mathbf{q}_a^{(t)}$ by (13);
 - 5 UKF localization step: $\mathbf{q}_c^{(t)}$ is updated from predicted $\mathbf{q}_c^{(t)}$ and $\sum_{m=0}^M \mathbf{b}_{si}^m$ by (12);
 - 6 $\mathbf{q}_a^{(t+1)}[0 : 3] = \mathbf{q}_c^{(t)}[0 : 3] + \mathbf{r}_{ca}$, $\mathbf{q}_a^{(t+1)}[3 : 5] = \mathbf{q}_c^{(t)}[3 : 5]$;
 - 7 return $\mathbf{q}_c^{(t)}, \mathbf{q}_a^{(t+1)}$;
-

III. EXPERIMENTS

The prototype implementation is shown in Fig. 5. The actuator is mounted at the end-effector of the Universal Robots UR3 robotic arm. The actuator consists of a DC motor and a N40 permanent magnet (diameter 24mm, length 18mm). Two permanent N38SH magnetic rings (both have an outer diameter of 12.8mm and inner diameter of 9mm,

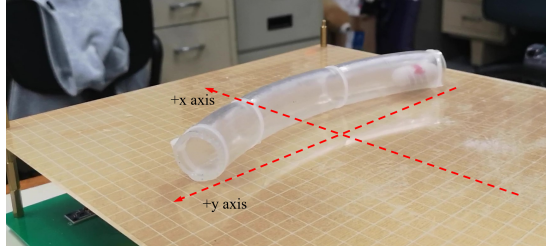


Fig. 6. Two experiments are conducted in the $+x$ and $+y$ directions, respectively.

and the lengths are 15mm and 5mm, respectively) are placed inside the capsule with a diameter of 16mm and a length of 35mm. There are 16 three-axis Honeywell MHC5883L magnetic sensors in the external sensor array, and the output frequency of each sensor is 60Hz.

In the first set of experiments, the capsule is actuated in a curved PVC tube with a length of 190mm and an inner diameter of 25mm, where the capsule's movement is restricted to translation along and rotation around the axis of the tube. As shown in Fig. 6, the capsule is actuated in the $+x$ and $+y$ directions in two experiments, respectively. As shown in Fig. 7, the estimated trajectory is almost consistent with the ground truth. Table I shows the localization accuracy of our proposed system in the above two experiments. The average errors in position and orientation are 5.5 ± 2.6 mm and 5.2 ± 4.3 °, respectively. Table II shows a detailed comparison between our proposed method and previous studies. As the first close-loop SMAL system based on rotating actuation

TABLE I

LOCALIZATION ACCURACY OF THE SYSTEM IN TWO EXPERIMENTS

metric	position (mm)				orientation (°)
	x	y	z	norm	
error	2.9	1.7	3.2	5.5	5.2
	\pm	\pm	\pm	\pm	\pm
	2.9	1.8	1.7	2.6	4.3

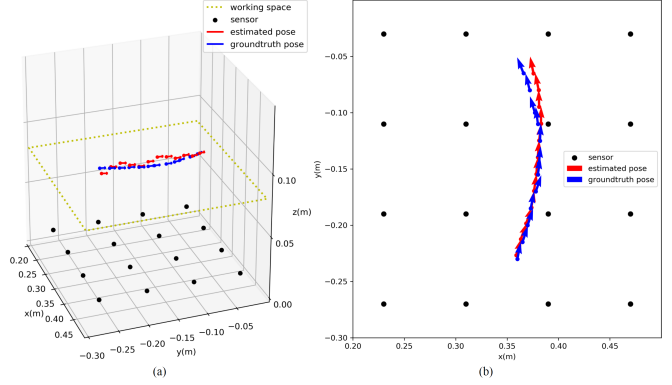


Fig. 7. The estimated trajectory of the moving capsule by our method (red arrows) is almost consistent with the ground truth (blue arrows).

and an external sensor array, our proposed method achieves a high localization accuracy.

In order to further investigate the robustness of the proposed system, we evaluate our method in experiments with more complex environments. In Fig. 8(a), the capsule moves in a curved PVC tube with a length of 190mm, which takes 49s and the average speed is 3.9mm/s. In Fig. 8(b), the capsule moves through a round PVC tube with a length of 419mm, which takes 284s and the average speed is 1.5mm/s. In Fig. 8(c), the capsule is actuated in a straight ex-vivo pig colon. It takes about 326s to move 240mm and the average speed is 0.74mm/s. In Fig. 8(d), the capsule moves through a curved ex-vivo pig colon with a length of 240mm, which takes about 329s and the average speed is 0.73mm/s. As is indicated from the results, both the shape and the material of the surrounding environment greatly affect the capsule's moving speed. With the same material, the round PVC tube reduces the speed by 61.5% compared to the curved one. With almost the similar shape, the ex-vivo pig colon with higher resistance reduces the speed by 81.03% compared to the PVC tube

TABLE II
COMPARISON BETWEEN PREVIOUS WORK AND PROPOSED METHOD

author	Guitron et al.[7]	Song et al.[13]	Popek et al.[8]	Tadese et al.[9]	Popek et al.[12]	Proposed Method
actuator	electromagnetic coil	dragging permanent magnet	rotating permanent magnet	dragging permanent magnet with electromagnetic coil	rotating permanent magnet	rotating permanent magnet
capsule structure	one magnet	one magnet	a cube magnet 6 sensors	a cube magnet 6 sensors	a cube magnet 6 sensors	two magnetic rings
capsule pose	2-D	5-D	6-D	6-D	6-D	5-D (miss the rotation angle θ)
sensor array	external	external	internal	internal	internal	external
close-loop	✓	by human eye	✓	✓	✓	✓
simultaneous	✗	by hand	✗	✓	✓	✓
speed (mm/s)	2.7 (plastic plane)	-	(straight line)	5.0 (straight line)	6.0 (straight line)	3.9 (straight line)
position error (mm)	1.0 ± 0.5	1.7	5.7 ± 3.0	< 5.0	8.5	5.5 ± 2.6
orientation error (°)	-	2.1	4.9 ± 2.4	< 6.0	7.1	5.2 ± 4.3

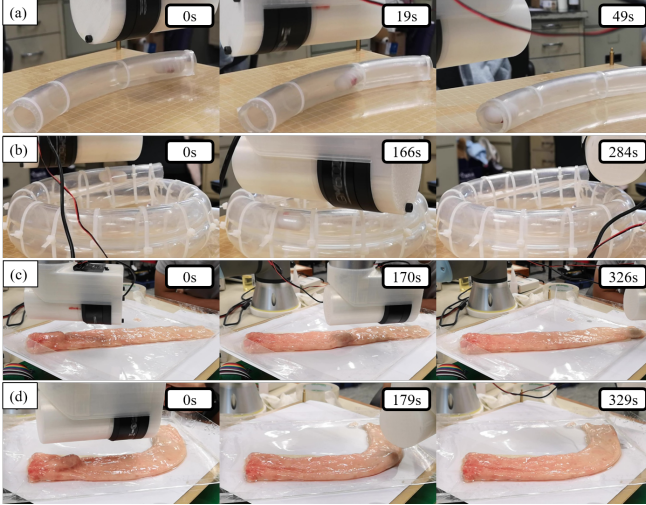


Fig. 8. Four experiments are conducted in different environments: (a) a curved PVC tube, (b) a round PVC tube, (c) a straight ex-vivo pig colon, and (d) a curved ex-vivo pig colon.

with lower resistance. The length of the human colon is about $1.5m$, so it is roughly estimated that it would take about 34.2min to finish the inspection if the speed of the capsule is assumed as 0.73mm/s . The manual inspection time of the current colonoscopy usually takes at least 30 minutes, while existing products for WCE requires above 8 hours to finish a whole imaging process. As a non-invasive and painless screening technique, our method only requires almost the same inspection time as the manual colonoscopy, thus is very prospective in the clinical applications. The complete experimental demonstrations of the proposed close-loop SMAL system in different environments can be found at <https://youtu.be/8vArgGvFrnw> or <https://www.bilibili.com/video/av74110171/>.

IV. CONCLUSIONS

In this paper, we build a close-loop simultaneous actuation and localization (SMAL) system for WCE. It is the first time the rotating actuation is combined with an external sensor array to accomplish the simultaneous actuation and localization of the capsule. As the magnetic actuation would introduce interferences with the localization system, we first propose a strategy to exploit the motion mode of the actuator and introduce the Integral Filter to eliminate the undesired magnetic field. Then the motion model of the moving capsule during actuation and localization is established to calculate the pose of the moving capsule. The Unscented Kalman Filter is utilized to fuse the actuation and localization steps to finally close the loop. The presented method is validated on both phantoms and ex-vivo pig colons. The localization errors of the capsule in position and orientation reach 5.5mm and 5.2° , respectively. Experimental results demonstrate that the accuracy of the proposed system is competitive with existing methods.

However, there remain some limitations to this work. The close-loop control is only effective when the capsule rotates synchronously with the actuator, and the moving speed of the capsule is strongly affected by the resistance of the surrounding environment. In the future work, the synchronization state of the capsule should be taken into consideration to ensure effective close-loop control of the system, and strategies should be proposed to adaptively change the magnetic torque of the actuator in different environment.

ACKNOWLEDGMENT

This project is partially supported by Shenzhen Science and Technology Innovation projects JCYJ20170413161503220 awarded to Max Q.-H. Meng.

REFERENCES

- [1] G. Iddan, G. Meron, A. Glukhovsky, and P. Swain, "Wireless capsule endoscopy," *Nature*, vol. 405, no. 6785, p. 417, 2000.
- [2] C. Hu, M. Q.-H. Meng, and M. Mandal, "Efficient magnetic localization and orientation technique for capsule endoscopy," *International Journal of Information Acquisition*, vol. 2, no. 01, pp. 23–36, 2005.
- [3] Y. Xu and M. Q.-H. Meng, "Free sensor array based relative localization system for wireless capsule endoscopy," in *2018 IEEE International Conference on Robotics and Biomimetics (ROBIO)*, pp. 550–555, IEEE, 2018.
- [4] S. Song, C. Hu, M. Li, W. Yang, and M. Q.-H. Meng, "Two-magnet-based 6d-localization and orientation for wireless capsule endoscope," in *2009 IEEE International Conference on Robotics and Biomimetics (ROBIO)*, pp. 2338–2343, IEEE, 2009.
- [5] S. Song, X. Qiu, W. Liu, and M. Q.-H. Meng, "An improved 6-d pose detection method based on opposing-magnet pair system and constraint multiple magnets tracking algorithm," *IEEE Sensors Journal*, vol. 17, no. 20, pp. 6752–6759, 2017.
- [6] F. Bianchi, A. Masaracchia, E. Shojaei Barjuei, A. Menciassi, A. Arezzo, A. Koulaouzidis, D. Stoyanov, P. Dario, and G. Ciuti, "Localization strategies for robotic endoscopic capsules: a review," *Expert review of medical devices*, vol. 16, no. 5, pp. 381–403, 2019.
- [7] S. Guirton, A. Guha, S. Li, and D. Rus, "Autonomous locomotion of a miniature, untethered origami robot using hall effect sensor-based magnetic localization," in *2017 IEEE International Conference on Robotics and Automation (ICRA)*, pp. 4807–4813, IEEE, 2017.
- [8] K. M. Popek, T. Schmid, and J. J. Abbott, "Six-degree-of-freedom localization of an untethered magnetic capsule using a single rotating magnetic dipole," *IEEE Robotics and Automation Letters*, vol. 2, no. 1, pp. 305–312, 2016.
- [9] A. Z. Taddei, P. R. Slawinski, M. Pirotta, E. De Momi, K. L. Obstein, and P. Valdastri, "Enhanced real-time pose estimation for closed-loop robotic manipulation of magnetically actuated capsule endoscopes," *The International journal of robotics research*, vol. 37, no. 8, pp. 890–911, 2018.
- [10] A. W. Mahoney and J. J. Abbott, "Generating rotating magnetic fields with a single permanent magnet for propulsion of untethered magnetic devices in a lumen," *IEEE Transactions on Robotics*, vol. 30, no. 2, pp. 411–420, 2013.
- [11] K. M. Miller, A. W. Mahoney, T. Schmid, and J. J. Abbott, "Proprioceptive magnetic-field sensing for closed-loop control of magnetic capsule endoscopes," in *2012 IEEE/RSJ International Conference on Intelligent Robots and Systems*, pp. 1994–1999, IEEE, 2012.
- [12] K. M. Popek, T. Hermans, and J. J. Abbott, "First demonstration of simultaneous localization and propulsion of a magnetic capsule in a lumen using a single rotating magnet," in *2017 IEEE International Conference on Robotics and Automation (ICRA)*, pp. 1154–1160, IEEE, 2017.
- [13] S. Song, X. Qiu, J. Wang, and M. Q.-H. Meng, "Real-time tracking and navigation for magnetically manipulated untethered robot," *IEEE Access*, vol. 4, pp. 7104–7110, 2016.